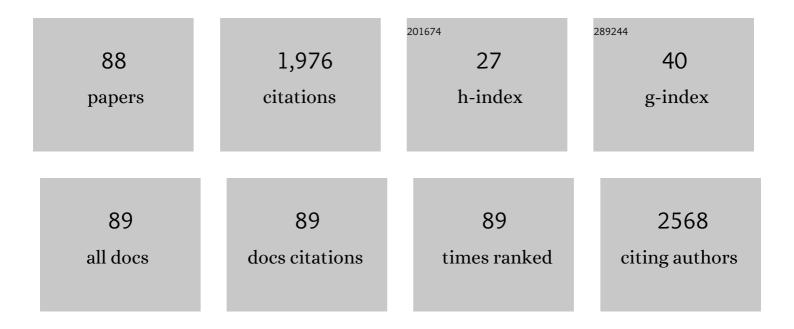
Faqin Dong

List of Publications by Year in descending order

Source: https://exaly.com/author-pdf/4946253/publications.pdf Version: 2024-02-01



FAOIN DONG

#	Article	IF	CITATIONS
1	Column bioleaching copper and its kinetics of waste printed circuit boards (WPCBs) by Acidithiobacillus ferrooxidans. Chemosphere, 2015, 141, 162-168.	8.2	106
2	Electrochemical oxidation of COD from real textile wastewaters: Kinetic study and energy consumption. Chemosphere, 2017, 171, 332-338.	8.2	93
3	Ti/PbO2-Sm2O3 composite based electrode for highly efficient electrocatalytic degradation of alizarin yellow R. Journal of Colloid and Interface Science, 2019, 533, 750-761.	9.4	85
4	Biosorption of uranium by Saccharomyces cerevisiae and surface interactions under culture conditions. Bioresource Technology, 2010, 101, 8573-8580.	9.6	84
5	In ³⁺ -doped BiVO ₄ photoanodes with passivated surface states for photoelectrochemical water oxidation. Journal of Materials Chemistry A, 2018, 6, 10456-10465.	10.3	83
6	Reduced graphene oxide-CoFe2O4 composites for supercapacitor electrode. Russian Journal of Electrochemistry, 2013, 49, 359-364.	0.9	60
7	Oxygen-doped activated carbons derived from three kinds of biomass: preparation, characterization and performance as electrode materials for supercapacitors. RSC Advances, 2016, 6, 5949-5956.	3.6	56
8	Improved Surface Charge Transfer in MoO3/BiVO4 Heterojunction Film for Photoelectrochemical Water Oxidation. Electrochimica Acta, 2017, 257, 181-191.	5.2	53
9	Poly(glycine)/graphene oxide modified glassy carbon electrode: Preparation, characterization and simultaneous electrochemical determination of dopamine, uric acid, guanine and adenine. Analytica Chimica Acta, 2018, 1031, 75-82.	5.4	50
10	Stable and tunable plasmon resonance of molybdenum oxide nanosheets from the ultraviolet to the near-infrared region for ultrasensitive surface-enhanced Raman analysis. Chemical Science, 2019, 10, 6330-6335.	7.4	50
11	Simultaneous removal and recovery of uranium from aqueous solution using TiO2 photoelectrochemical reduction method. Journal of Radioanalytical and Nuclear Chemistry, 2017, 313, 59-67.	1.5	47
12	Optimized terbium doped Ti/PbO2 dimensional stable anode as a strong tool for electrocatalytic degradation of imidacloprid waste water. Ecotoxicology and Environmental Safety, 2020, 188, 109921.	6.0	46
13	Phenolic endocrine disrupting chemicals in an urban receiving river (Panlong river) of Yunnan–Guizhou plateau: Occurrence, bioaccumulation and sources. Ecotoxicology and Environmental Safety, 2016, 128, 133-142.	6.0	45
14	Spectroscopic study on biological mackinawite (FeS) synthesized by ferric reducing bacteria (FRB) and sulfate reducing bacteria (SRB): Implications for in-situ remediation of acid mine drainage. Spectrochimica Acta - Part A: Molecular and Biomolecular Spectroscopy, 2017, 173, 544-548.	3.9	41
15	Co/Sm-modified Ti/PbO2 anode for atrazine degradation: Effective electrocatalytic performance and degradation mechanism. Chemosphere, 2021, 268, 128799.	8.2	41
16	Magnetic Field-Assisted Photoelectrochemical Water Splitting: The Photoelectrodes Have Weaker Nonradiative Recombination of Carrier. ACS Catalysis, 2021, 11, 1242-1247.	11.2	41
17	Qinghai–tibetan plateau peatland sustainable utilization under anthropogenic disturbances and climate change. Ecosystem Health and Sustainability, 2017, 3, .	3.1	40
18	Effect of glycerol on the preparation of phosphogypsum-based CaSO4·0.5H2O whiskers. Journal of Materials Science, 2014, 49, 1957-1963.	3.7	38

#	Article	IF	CITATIONS
19	Coal tar residues-based nanostructured activated carbon/Fe3O4 composite electrode materials for supercapacitors. Journal of Solid State Electrochemistry, 2014, 18, 665-672.	2.5	38
20	Microscopic and Spectroscopic Insights into Uranium Phosphate Mineral Precipitated by <i>Bacillus Mucilaginosus</i> . ACS Earth and Space Chemistry, 2017, 1, 483-492.	2.7	38
21	Enhancing As(V) adsorption and passivation using biologically formed nano-sized FeS coatings on limestone: Implications for acid mine drainage treatment and neutralization. Chemosphere, 2017, 168, 529-538.	8.2	34
22	Biosorption of Strontium from Simulated Nuclear Wastewater by Scenedesmus spinosus under Culture Conditions: Adsorption and Bioaccumulation Processes and Models. International Journal of Environmental Research and Public Health, 2014, 11, 6099-6118.	2.6	33
23	Enhanced Photoelectrochemical Water Oxidation Performance on BiVO ₄ by Coupling of CoMoO ₄ as a Hole-Transfer and Conversion Cocatalyst. ACS Applied Materials & Interfaces, 2018, 10, 42207-42216.	8.0	33
24	Adsorption of arsenic(V) on bone char: batch, column and modeling studies. Environmental Earth Sciences, 2014, 72, 2081-2090.	2.7	32
25	Objective Findings on the K-Doped <i>g</i> -C ₃ N ₄ Photocatalysts: The Presence and Influence of Organic Byproducts on K-Doped <i>g</i> -C ₃ N ₄ Photocatalysis. Langmuir, 2021, 37, 4859-4868.	3.5	32
26	The role of nano-sized manganese coatings on bone char in removing arsenic(V) from solution: Implications for permeable reactive barrier technologies. Chemosphere, 2016, 153, 146-154.	8.2	31
27	Dimensionally stable Ti/SnO2-RuO2 composite electrode based highly efficient electrocatalytic degradation of industrial gallic acid effluent. Chemosphere, 2019, 224, 707-715.	8.2	31
28	Kinetics and pH-dependent uranium bioprecipitation by Shewanella putrefaciens under aerobic conditions. Journal of Radioanalytical and Nuclear Chemistry, 2017, 312, 531-541.	1.5	30
29	Thermal decomposition based fabrication of dimensionally stable Ti/SnO2–RuO2 anode for highly efficient electrocatalytic degradation of alizarin cyanin green. Chemosphere, 2020, 261, 128201.	8.2	27
30	Efficient extraction of U(VI) from uranium enrichment process wastewater by amine-aminophosphonate-modified polyacrylonitrile fibers. Science of the Total Environment, 2022, 831, 154743.	8.0	24
31	Boosted Water Oxidation Activity and Kinetics on BiVO4 Photoanodes with Multihigh-Index Crystal Facets. Inorganic Chemistry, 2018, 57, 15280-15288.	4.0	22
32	Photoelectrochemical driving and clean synthesis of energetic salts of 5,5′-azotetrazolate at room temperature. Green Chemistry, 2018, 20, 3722-3726.	9.0	22
33	Programmed gradient descent biosorption of strontium ions by Saccaromyces cerevisiae and ashing analysis: A decrement solution for nuclide and heavy metal disposal. Journal of Hazardous Materials, 2016, 314, 295-303.	12.4	21
34	Electrocatalytic degradation of bromocresol green wastewater on Ti/SnO2-RuO2 electrode. Water Science and Technology, 2017, 75, 220-227.	2.5	21
35	Contribution of surface functional groups and interface interaction to biosorption of strontium ions by Saccharomyces cerevisiae under culture conditions. RSC Advances, 2017, 7, 50880-50888.	3.6	20
36	MoO3/BiVO4 heterojunction film with oxygen vacancies for efficient and stable photoelectrochemical water oxidation. Journal of Materials Science, 2019, 54, 671-682.	3.7	20

#	Article	IF	CITATIONS
37	Direct Blue Light-Induced Autocatalytic Oxidation of <i>o</i> -Phenylenediamine for Highly Sensitive Visual Detection of Triaminotrinitrobenzene. Analytical Chemistry, 2019, 91, 6155-6161.	6.5	19
38	Spectroscopic evidence and molecular simulation investigation of the bonding interaction between lysine and montmorillonite: Implications for the distribution of soil organic nitrogen. Applied Clay Science, 2018, 159, 3-9.	5.2	18
39	Polychlorinated biphenyls and organochlorine pesticides in atmospheric particulate matter of Northern China: distribution, sources, and risk assessment. Environmental Science and Pollution Research, 2015, 22, 17171-17181.	5.3	17
40	Preparation of Calcium Sulfate Hemihydrate and Application in Polypropylene Composites. Journal of Nanoscience and Nanotechnology, 2017, 17, 6970-6975.	0.9	17
41	Characteristics and mechanism of uranium photocatalytic removal enhanced by chelating hole scavenger citric acid in a TiO2 suspension system. Journal of Radioanalytical and Nuclear Chemistry, 2019, 319, 147-158.	1.5	16
42	Preparation of Anhydrous Calcium Sulfate Whiskers from Phosphogypsum in H ₂ O-H ₂ SO ₄ Autoclave-Free Hydrothermal System. Materials Transactions, 2017, 58, 1111-1117.	1.2	15
43	Simultaneous voltammetric determination of guanine and adenine by using a glassy carbon electrode modified with a composite consisting of carbon quantum dots and overoxidized poly(2-aminopyridine). Mikrochimica Acta, 2018, 185, 107.	5.0	15
44	Microbially Mediated Stable Uranium Phosphate Nano-Biominerals. Journal of Nanoscience and Nanotechnology, 2017, 17, 6771-6780.	0.9	14
45	Cobalt disulfide nanosphere dispersed on multi-walled carbon nanotubes: an efficient and stable electrocatalyst for hydrogen evolution reaction. Ionics, 2018, 24, 3591-3599.	2.4	14
46	Threshold displacement energies and displacement cascades in 4H-SiC: Molecular dynamic simulations. AIP Advances, 2019, 9, .	1.3	14
47	Improving photoelectrochemical reduction of Cr(VI) ions by building α-Fe2O3/TiO2 electrode. Environmental Science and Pollution Research, 2018, 25, 22455-22463.	5.3	13
48	A glassy carbon electrode modified with a nanocomposite consisting of carbon nanohorns and poly(2-aminopyridine) for non-enzymatic amperometric determination of hydrogen peroxide. Mikrochimica Acta, 2016, 183, 3237-3242.	5.0	12
49	Nanosized Fe3O4-modified activated carbon for supercapacitor electrodes. Russian Journal of Electrochemistry, 2013, 49, 354-358.	0.9	11
50	Novel one-pot hydrothermal fabrication of cuprous oxide-attapulgite/graphene for non-enzyme glucose sensing. Analytical Methods, 2015, 7, 2747-2753.	2.7	11
51	Enhanced Electrocatalytic Activity of Dual Template Based Pt/Cuâ€zeolite A/Graphene for Methanol Electrooxidation. Chinese Journal of Chemistry, 2018, 36, 37-41.	4.9	11
52	Ordered NiO-TiO ₂ nanotube arrays as an efficient catalyst support for methanol oxidation. Physica Status Solidi (A) Applications and Materials Science, 2015, 212, 2085-2090.	1.8	10
53	Synergistic interface behavior of strontium adsorption using mixed microorganisms. Environmental Science and Pollution Research, 2018, 25, 22368-22377.	5.3	9
54	Chemically modified mesoporous wood: a versatile sensor for visual colorimetric detection of trinitrotoluene in water, air, and soil by smartphone camera. Analytical and Bioanalytical Chemistry, 2019, 411, 8063-8071.	3.7	9

#	Article	IF	CITATIONS
55	Tailored manganese hexacyanoferrate/graphene oxide nanocomposites: one-pot facile synthesis and favorable capacitance behavior for supercapacitors. Journal of Materials Science: Materials in Electronics, 2020, 31, 2720-2728.	2.2	9
56	Altering the substituents of salicylic acid to improve Berthelot reaction for ultrasensitive colorimetric detection of ammonium and atmospheric ammonia. Analytical and Bioanalytical Chemistry, 2021, 413, 5695-5702.	3.7	9
57	Organic acid mediated photoelectrochemical reduction of U(<scp>vi</scp>) to U(<scp>iv</scp>) in waste water: electrochemical parameters and spectroscopy. RSC Advances, 2021, 11, 23241-23248.	3.6	9
58	Mechanochemical Synthesis of Defective Molybdenum Trioxide, Titanium Dioxide, and Zinc Oxide at Room Temperature. ACS Sustainable Chemistry and Engineering, 0, , .	6.7	8
59	Nanobiocatalyst consisting of immobilized α-amylase on montmorillonite exhibiting enhanced enzymatic performance based on the allosteric effect. Colloids and Surfaces B: Biointerfaces, 2022, 211, 112290.	5.0	8
60	Effect of Additives on Calcium Sulfate Hemihydrate Whiskers Morphology from Calcium Sulfate Dehydrate and Phosphogypsum. Materials and Manufacturing Processes, 2016, 31, 2037-2043.	4.7	7
61	Bifunctional nanozyme of copper organophyllosilicate for the ultrasensitive detection of hydroquinone. Analytical and Bioanalytical Chemistry, 2022, 414, 1039-1048.	3.7	7
62	Infrared and Raman spectroscopic characterizations on new Fe sulphoarsenate hilarionite (Fe2(III)(SO4)(AsO4)(OH)·6H2O): Implications for arsenic mineralogy in supergene environment of mine area. Spectrochimica Acta - Part A: Molecular and Biomolecular Spectroscopy, 2017, 170, 9-13.	3.9	6
63	Synergistic effects of electron shuttle AQS and Alcaligenes faecalis on photocatalytic removal of U(VI). Journal of Radioanalytical and Nuclear Chemistry, 2019, 322, 731-742.	1.5	6
64	Tiankeng: an ideal place for climate warming research on forest ecosystems. Environmental Earth Sciences, 2019, 78, 1.	2.7	6
65	Influence of troilite on the decomposition of ammonium jarosite and estimated activation energy. Journal of Thermal Analysis and Calorimetry, 2020, 139, 933-939.	3.6	6
66	Recovery elemental sulfur from calcium sulfide prepared by red gypsum in sulfuric acid wastewater treatment. Journal of Material Cycles and Waste Management, 2022, 24, 1542-1550.	3.0	6
67	Design and construction of copper-containing organophyllosilicates as laccase-mimicking nanozyme for efficient removal of phenolic pollutants. Journal of Materials Science, 2022, 57, 10084-10099.	3.7	6
68	In vitro genotoxicity of asbestos substitutes induced by coupled stimulation of dissolved high-valence ions and oxide radicals. Environmental Science and Pollution Research, 2018, 25, 22356-22367.	5.3	5
69	CTAB-assisted microemulsion synthesis of unique 3D network nanostructured polypyrrole presenting significantly diverse capacitance performances in different electrolytes. Journal of Materials Science: Materials in Electronics, 2018, 29, 17552-17562.	2.2	5
70	Facile preparation of high-strength α-CaSO4·0.5H2O regulated by maleic acid from phosphogypsum: experimental and molecular dynamics simulation studies. SN Applied Sciences, 2020, 2, 1.	2.9	5
71	Highly Efficient Removal of Congo Red from Aqueous Solution by Limeâ€Preconditioned Phosphogypsum. ChemistrySelect, 2022, 7, .	1.5	5
72	Remarkably enhanced activity of 4A zeolite modified Pt/reduced graphene oxide electrocatalyst towards methanol electrooxidation in alkaline medium. Ionics, 2019, 25, 5131-5140.	2.4	4

#	Article	IF	CITATIONS
73	Interface interaction between high-siliceous/calcareous mineral granules and model cell membranes dominated by electrostatic force. Environmental Science and Pollution Research, 2021, 28, 27432-27445.	5.3	4
74	Objective Observations of the Electrochemical Production of H ₂ O ₂ in KHCO ₃ Aqueous Electrolyte and Related Application Inspirations. Journal of Physical Chemistry C, 2021, 125, 19831-19838.	3.1	4
75	Novel 3D cross-shaped Zn/Co bimetallic zeolite imidazolate frameworks for simultaneous removal Cr(VI) and Congo Red. Environmental Science and Pollution Research, 2022, 29, 40041-40052.	5.3	4
76	The interface interaction behavior between E. coli and two kinds of fibrous minerals. Environmental Science and Pollution Research, 2018, 25, 22420-22428.	5.3	3
77	Meta-analysis of experimental warming on soil invertase and urease activities. Acta Agriculturae Scandinavica - Section B Soil and Plant Science, 2018, 68, 104-109.	0.6	3
78	Accurate Understanding the Catalytic Role of MnO2 in the Oxidative-Coupling of 2-naphthols into 1,1′-bi-2-naphthols. Catalysis Letters, 2021, 151, 901-908.	2.6	3
79	Mussel Inspired Modification of Rubber Crumbs for Improved Interfacial Adhesion in Rubber Cement Mortar. Applied Composite Materials, 2021, 28, 1767-1780.	2.5	3
80	Characterization of the dissolution of tooeleite under <i>Acidithiobacillus ferrooxidans</i> relevant to mineral trap for arsenic removal. Desalination and Water Treatment, 2016, 57, 15108-15114.	1.0	2
81	Synergistic Oxidative Stress of Surface Silanol and Hydroxyl Radical of Crystal and Amorphous Silica in A549 Cells. Journal of Nanoscience and Nanotechnology, 2017, 17, 6645-6654.	0.9	2
82	Preparation of Pyrrhotite from Ammonium Jarosite and Estimation of Activation Energy in Reducing Atmosphere. International Journal of Chemical Reactor Engineering, 2019, 17, .	1.1	2
83	Influence of Carbon and Pyrite on Desulfurization Behavior of Red Gypsum at High Temperature. Journal of Sustainable Metallurgy, 2022, 8, 409-418.	2.3	2
84	Powder Quartz/Nano-TiO2 Composite: Mechanochemical Preparation and Photocatalytic Degradation of Formaldehyde. Journal Wuhan University of Technology, Materials Science Edition, 2018, 33, 1381-1386.	1.0	1
85	Gadolinium chloride promotes proliferation of HEK293 human embryonic kidney cells by activating EGFR/PI3K/Akt and MAPK pathways. BioMetals, 2019, 32, 683-693.	4.1	1
86	CONSTRUCTION AND CHARACTERIZATION OF A NANOSTRUCTURED BIOCATALYST CONSISTING OF IMMOBILIZED LIPASE ON Mg-AMINO-CLAY. Clays and Clay Minerals, 2021, 69, 434-442.	1.3	1
87	Interface effect of ultrafine mineral particles and microorganisms. Environmental Science and Pollution Research, 2018, 25, 22323-22327.	5.3	0
88	Transformation of radionuclide occurrence state in uranium and strontium recycling by Saccharomyces cerevisiae. Journal of Radioanalytical and Nuclear Chemistry, 0, , .	1.5	0